

Article

Characteristics and Provenance Implications of Rare Earth Elements and Nd Isotope in PM_{2.5} in a Coastal City of Southeastern China

Yihong Li ¹, Shanshan Wang ^{2,3}, Yu Yan ^{1,2}, Jinpei Yan ^{2,3} , Ruilian Yu ^{1,*} and Gongren Hu ^{1,4,*}¹ College of Chemical Engineering, Huaqiao University, Xiamen 361021, China² Key Laboratory of Global Change and Marine Atmospheric Chemistry, Ministry of Natural Resources, Xiamen 361005, China³ Third Institute of Oceanography, Ministry of Natural Resources, Xiamen 361005, China⁴ Institute of Environmental and Ecological Engineering, Huaqiao University, Xiamen 361021, China

* Correspondence: ruiliany@hqu.edu.cn (R.Y.); grhu@hqu.edu.cn (G.H.); Tel.: +86-592-6162300 (R.Y. & G.H.)

Abstract: The source apportionment of fine particulate matters, especially PM_{2.5}, has drawn great attention worldwide. Since rare earth elements (REEs) and Nd isotopes can serve as source tracers, in this study, the characteristics and provenance implications of REEs and Nd isotopes in PM_{2.5} of four seasons in Xiamen city, China, were investigated. The range of the ratios of Σ REE to PM_{2.5} was 1.04×10^{-5} to 8.06×10^{-4} , and the mean concentration of REEs in PM_{2.5} were in the order of spring > autumn > winter > summer. According to the geoaccumulation index (I_{geo}), spring was the season in which anthropogenic sources had the greatest impact on the REEs in PM_{2.5}. The chondrite-normalized REE distribution patterns exhibited light rare earth elements (LREEs, including La, Ce, Pr, Nd, Pm, Sm and Eu) enrichment and a flat heavy rare earth elements (HREEs, including Gd, Tb, Dy, Ho, Er, Tm, Yb and Lu) pattern. Significant negative Eu anomalies and no significant Ce anomalies were observed in the PM_{2.5}. The results of La-Ce-Sm ternary plots indicated that the REEs in the PM_{2.5} might be related to both natural and anthropogenic sources. Combined with the Nd isotope, the ¹⁴³Nd/¹⁴⁴Nd versus Ce/Ce* plot further illustrated that the REEs in the PM_{2.5} seemed to mostly originate from multiple potential sources, in which vehicle exhaust emissions, coal burning and cement dust made a great contribution to REEs in PM_{2.5}.

Keywords: PM_{2.5}; rare earth elements; Nd isotope; source analysis

Citation: Li, Y.; Wang, S.; Yan, Y.; Yan, J.; Yu, R.; Hu, G. Characteristics and Provenance Implications of Rare Earth Elements and Nd Isotope in PM_{2.5} in a Coastal City of Southeastern China.

Atmosphere **2022**, *13*, 1367. <https://doi.org/10.3390/atmos13091367>

Academic Editors: Jun Li and Zhixiong Li

Received: 26 July 2022

Accepted: 23 August 2022

Published: 26 August 2022

Publisher's Note: MDPI stays neutral with regard to jurisdictional claims in published maps and institutional affiliations.



Copyright: © 2022 by the authors. Licensee MDPI, Basel, Switzerland. This article is an open access article distributed under the terms and conditions of the Creative Commons Attribution (CC BY) license (<https://creativecommons.org/licenses/by/4.0/>).

1. Introduction

Hazy weather has occurred frequently in recent years and aroused great concern across the world [1–5]. Haze is generally caused by fine atmospheric particulate matter (PM), especially particulates with the aerodynamic diameters of less than 2.5 μ m (PM_{2.5}) [6]. PM_{2.5} can not only cause environmental problems but also enter the alveoli directly and harm human health [7,8]. PM_{2.5} stays in the atmosphere for a long time and can be transported over long distances, leading to widespread pollution events [9,10]. PM_{2.5} in cities is not only complex in composition but also comes from various sources, such as coal burning, vehicle exhaust, road dust, industrial emissions, construction activities, waste incineration and soil dust [11,12]. The sources of PM need to be identified for the control and prevention of atmospheric PM pollution.

Rare earth elements (REEs), which are also known as lanthanoid elements, generally could be divided into light rare earth elements (LREEs, including La, Ce, Pr, Nd, Pm, Sm and Eu) and heavy rare earth elements (HREEs, including Gd, Tb, Dy, Ho, Er, Tm, Yb and Lu). REEs with special physical and chemical characteristics are often used as tracer elements in source apportionment because REEs are not easily affected by weathering, migration, transformation and sedimentation [13,14]. Furthermore, previous studies have

shown that REEs can accumulate in the hair, blood, brain, bone, liver and lung and other human tissues, causing irreversible harm to the human nervous system, respiratory system, digestive system, liver function, renal function, and so on [15–19]. Although the concentrations of REEs in PM_{2.5} may only account for a low proportion, REEs still pose a potential threat to human health [20]. Therefore, the REEs in PM_{2.5} should be more effectively controlled by understanding the characteristics and provenances of REEs in PM_{2.5}.

Neodymium (Nd) isotope composition has also proved to be a powerful and sensitive tracer [21] and is used for source apportionment due to its stable existence in the atmosphere and difficulty in fractionation [22–24]. As one of the REEs, Nd is found in nature in two major isotopes, namely ¹⁴⁴Nd and ¹⁴³Nd. The ratio of ¹⁴³Nd/¹⁴⁴Nd has been usually measured to more accurately explain the source, migration and transformation of REEs [25–27]. In particular, the combination of ¹⁴³Nd/¹⁴⁴Nd and REE characteristics was successfully used to determine the sources of REEs in atmospheric particulates [28–30]. For example, our previous study investigated the provenance implications of REEs and Sr-Nd isotopes in PM_{2.5} aerosols and PM_{2.5} fugitive dusts from Nanchang city, China [29]. However, there are still few studies that have systematically analyzed the temporal sources of PM_{2.5} using the combination of REE characteristics and Nd isotope.

China has relatively abundant REE reserves and is a major producer of REEs [31,32]. REEs are widely used in some high-tech industries such as electronics, pharmaceuticals, petrochemical, metallurgy, glass and ceramics, machinery, energy, photoelectric industry, environmental protection, agriculture and other fields and widely exist in the environment [33,34]. Xiamen city (24°23′–24°54′ N, 117°53′–118°26′ E) is a typical coastal city in southeastern China. Some high-tech industries that consume REEs, such as electronics and biopharmaceuticals, are well developed in Xiamen city [35]. Although the atmospheric environmental quality in Xiamen is among the best in China when compared with other cities with serious air pollution, there is still a huge gap compared with other countries, such as Japan, the United States and most European countries [36,37]. Previously, many experts and scholars mainly focused on the atmospheric PM_{2.5} pollution in China's northern regions with severe smog and rare earth mining areas. To date, there have also been some studies on atmospheric PM_{2.5} in Xiamen [38–44]. However, the use of the characteristics and provenances of REEs and Nd isotope to determine the origins of PM_{2.5} in this coastal city is quite limited. Therefore, this study aims to analyze the characteristics and provenance implications of REEs and Nd isotope in PM_{2.5} throughout the year in Xiamen city, in order to provide reliable data support and a scientific basis for the prevention and control of atmospheric PM_{2.5} pollution.

2. Materials and Methods

2.1. Study Area

Xiamen city covers a land area of 1699 km² and a sea area of 390 km², and it is an important marine port city located in the southeast of China. Xiamen has a monsoonal humid subtropical climate, with hot and humid summer and mild and dry winter. The dominant wind direction is southeast in spring and summer, and northeast in autumn and winter. Xiamen can be divided into two parts: urban areas including Siming and Huli districts, and suburban areas consisting of Haicang, Jimei, Tong'an and Xiang'an districts. Urban areas are mostly residential and commercial areas with large population density and vehicle flow, while industries are mostly distributed in suburban areas.

As described in our previous study in detail, sampling sites of PM_{2.5} were set up in both urban and suburban areas of Xiamen city, with the urban and suburban sampling sites located in Siming and Jimei districts, respectively [45]. Both urban and suburban sampling sites were located on the building roof and about 20 m above ground. The seasonal PM_{2.5} samples were collected in spring (8 April–1 May 2017), summer (8 August–26 August 2017), autumn (10 October 10–27 October 2018) and winter (27 December 2018–13 January 2019)

except on bad weather days. For each season, 17 samples were collected in urban and suburban areas, respectively.

2.2. Sampling and Preparation

The PM_{2.5} samples were collected by using TH-150A intelligent volumetric samplers (Wuhan Tianhong Intelligent Instruments, Inc., Wuhan, China) with a sampling flow of 100 L min⁻¹. Sampling was conducted for a total of 22 h from 8:00 a.m. to 6:00 a.m. of the next day. Polytetrafluoroethylene membranes with a diameter of 90 mm (Whatman) were used for PM_{2.5} sampling. Prior to sampling, the membranes were placed in a clean chamber at constant temperature (25 ± 1 °C) and relative humidity (52 ± 2%) for at least 48 h to attain constant weight before and after sampling. The membranes were weighed using an electronic scale with an accuracy of 0.01 mg (Sartorius T-114). The concentrations of PM_{2.5} were determined by the ratio of the weight difference before and after sampling to the total sampling volume. All PM_{2.5} samples were wrapped in aluminum foil, placed in sealed bags, and stored in a refrigerator at −20 °C for testing.

Meanwhile, in order to investigate the provenances of REEs in PM_{2.5}, the main potential source materials, including gasoline and diesel vehicle exhaust dust, coal burning dust, cement dust, road dust, steel dust, waste incineration dust, firework and firecracker dust and background soil, were also collected. Vehicle exhaust dust was collected from the exhaust pipes of gasoline vehicles and diesel vehicles, and a total of six samples were collected. A total of seven samples were collected for electrostatic dust removal in Xiamen raw coal fly ash furnace bottom slag coal-fired power plant. Five samples of the waste incineration dust were collected from the dust falling around the waste incineration plant. Cement dust was collected at the construction site near the sampling point; samples of fireworks and firecrackers were taken at the place after discharge; and six samples of cement dust and firework dust were collected, respectively. Road dust was collected from the roadside, and dust was collected from leaves, wooden doors, windows and glass surfaces, and six samples were collected. All the potential source samples were brushed into sealed bags with clean brushes, labeled and stored in a refrigerator at −20 °C for testing.

2.3. Analysis Method and Quality Assurance

The HNO₃-HF method was employed for digestion [30], and a mass spectrometer with inductively coupled plasma was used to measure the REE concentrations (ICP-MS; ELAN 9000, PerkinElmer, Waltham, MA, USA). Reagent blanks and blank filters using the same digestion were also processed, and both had a minimal impact on the REE determination. For quality assurance, the Institute of Geophysical and Geochemical Exploration (China) accredited soil reference material GSS-5 was employed. The recovery rate of the determined elements was in the range of 80–120%, and the relative standard deviation (RSD) was less than 5%. Fourteen rare earth elements were detected, the detection limits for REEs were 0.002 µg/g to 0.006 µg/g. The relative standard deviation was less than 5.0%, and the recoveries were within 91.3% to 106.7%.

The samples were additionally digested as described for the determination of REEs in order to analyze the Nd isotopic compositions. When the digestion solution was dried, 1.5 mL of 7.2 mol L⁻¹ excellent-grade pure hydrochloric acid was added. Then, the solution was evaporated, and 1.5 mL of 0.5 mol L⁻¹ hydrochloric acid was added again. After centrifuging, the elution was transferred into CL-P507 resin, and 3 mL of 0.1 mol L⁻¹ hydrochloric acid was utilized once more for the separation and purification of Nd. The Nd isotopes were measured using a thermal ionization mass spectrometer (TI-MS). The Nd isotopic compositions of reference materials (JNdi-1) were examined to verify the repeatability and precision of Nd isotope determination. The measured ¹⁴³Nd/¹⁴⁴Nd value for the JNdi-1 standard was 0.512118 ± 0.000020, which was coincident with the referenced value of 0.512148 ± 0.000029 (n = 6) [30].

3. Results and Discussion

3.1. REE Concentrations in PM_{2.5}

The concentrations of REEs in PM_{2.5} in Xiamen are shown in Figure 1 and Table 1. The range of the ratios of Σ REE to PM_{2.5} was 1.04×10^{-5} to 8.06×10^{-4} , with the mean concentrations following the order of spring > autumn > winter > summer. The mean concentrations of Σ REE were suburban > urban in spring and summer, whereas they were urban > suburban in autumn and winter. This result indicated that the REEs in PM_{2.5} might be affected by different potential sources in different seasons. The mean concentrations of Σ LREE and Σ HREE ranged from 0.35 to 42.83 ng/m³ and 0.03 to 3.56 ng/m³, respectively. The spatial and temporal distribution characteristics of Σ LREE and Σ HREE in different seasons were consistent with those of Σ REE. Furthermore, the Σ REE of PM_{2.5} in Xiamen in this study were obviously lower than those collected in Nanchang [29,46] and Daqing [47] but similar to those in Quanzhou [48].

Table 1. Mean concentrations (ng/m³) of Σ LREE, Σ HREE and Σ REE in PM_{2.5} and the ratios of Σ REE to PM_{2.5} in Xiamen city.

	Spring		Summer		Autumn		Winter	
	Urban	Suburban	Urban	Suburban	Urban	Suburban	Urban	Suburban
Σ LREE	20.38	42.83	1.13	2.12	2.31	1.64	2.1	0.59
Σ HREE	1.92	3.56	0.12	0.2	0.19	0.19	0.2	0.07
Σ REE	22.3	46.4	1.25	2.33	2.5	1.83	2.29	0.65
Σ REE/PM _{2.5} × 10 ⁻⁵	36.31	80.58	4.07	6.33	5.68	3.76	5.37	1.92

The mean concentrations (ng/m³) of each REE in PM_{2.5} in Xiamen city showed an enrichment of the LREEs in the order of Ce > La > Nd > Pr > Sm > Gd > Dy > Yb > Er > Eu > Tb > Ho > Tm > Lu. The order of REEs in the PM_{2.5} samples mostly complied with the Oddo–Harkins rule but did not exactly match that in the local background soil (Ce > La > Nd > Pr > Sm > Gd > Dy > Yb > Er > Eu > Ho > Tb > Lu > Tm), suggesting that anthropogenic activities had some influence on the REEs in the PM_{2.5} samples. In order to assess the anthropogenic impact, the geoaccumulation index (I_{geo}) was further applied.

3.2. REEs' Geoaccumulation Indices in the PM_{2.5}

I_{geo} , which was originally introduced by Müller [49], was calculated as $I_{geo} = \log_2[C_n/(1.5B_n)]$, where C_n denotes the concentrations of REEs in the sample, and B_n is the background value. $I_{geo} \leq 0$ is regarded as primarily affected by natural sources. Otherwise, the $I_{geo} > 0$ indicates to a certain extent of the impact of anthropogenic activities. $I_{geo} > 0$ could be divided into different levels of impact: No influence/moderate influence ($0 < I_{geo} \leq 1$). Moderate influence ($1 < I_{geo} \leq 2$). Moderate influence/strong influence ($2 < I_{geo} \leq 3$). Strong influence ($3 < I_{geo} \leq 4$). Strong influence/extreme influence ($4 < I_{geo} \leq 5$). Extreme influence ($I_{geo} > 5$). The I_{geo} values of the REEs are illustrated in Figure 2. With the exception of spring, the median I_{geo} values of REEs in the PM_{2.5} samples were almost less than 0 in most seasons, demonstrating that anthropogenic sources primarily impacted the REEs in PM_{2.5} in the spring. The I_{geo} assessment showed that the fourteen rare earth elements were moderately or strongly influential in spring in urban and suburban areas, while the other seasons had no influence or moderate influence. This might be because of higher wind speed, which can increase the ground floating dust and then result in the accumulation of REEs in PM_{2.5} in spring. Furthermore, when analyzing the I_{geo} values of PM_{2.5} for each season in detail, the median I_{geo} values were higher in suburban than in urban areas in spring and summer, while opposite was true in autumn and winter, which suggested different sources in different seasons.

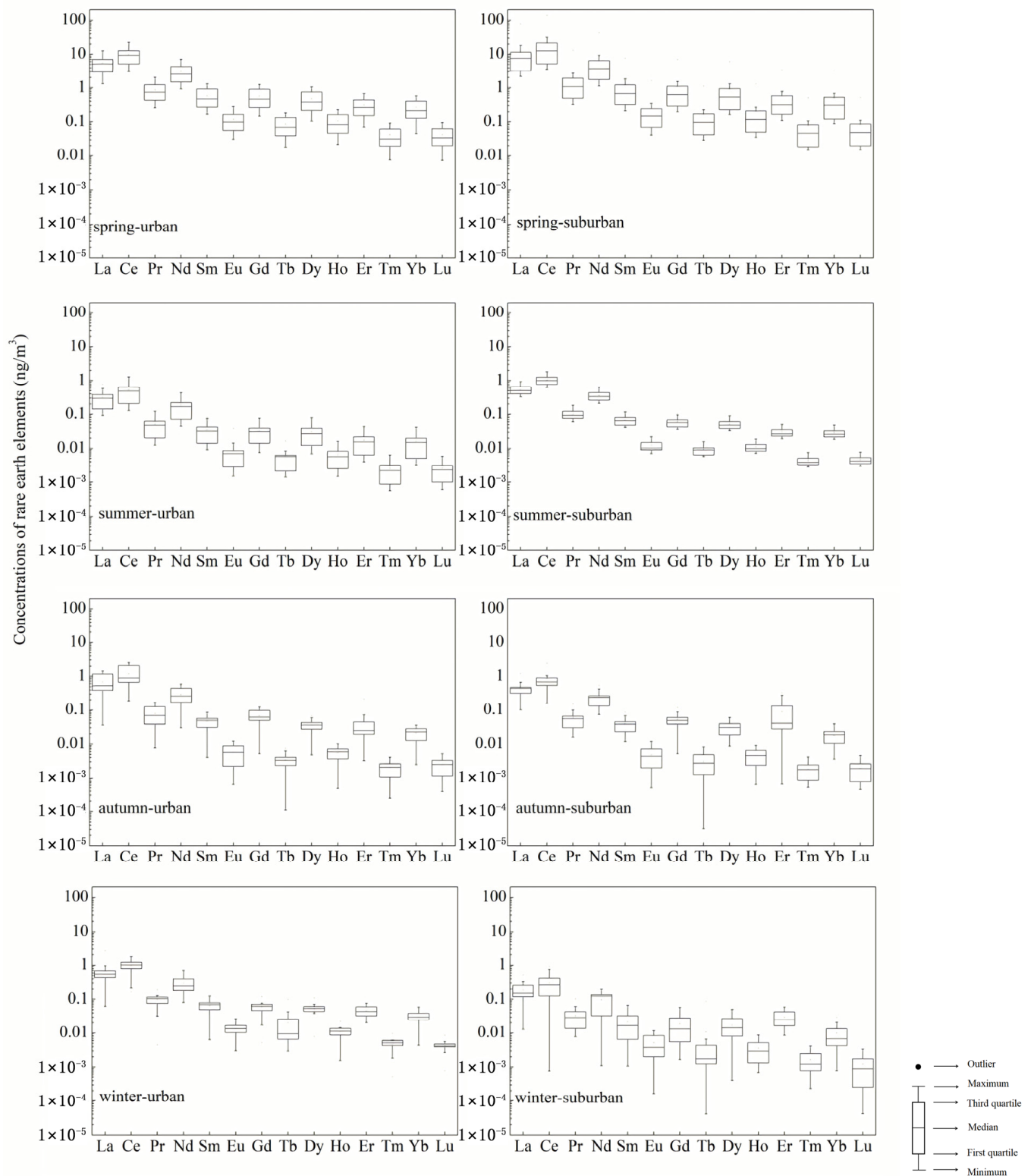


Figure 1. The concentrations of REEs in PM_{2.5} in Xiamen.

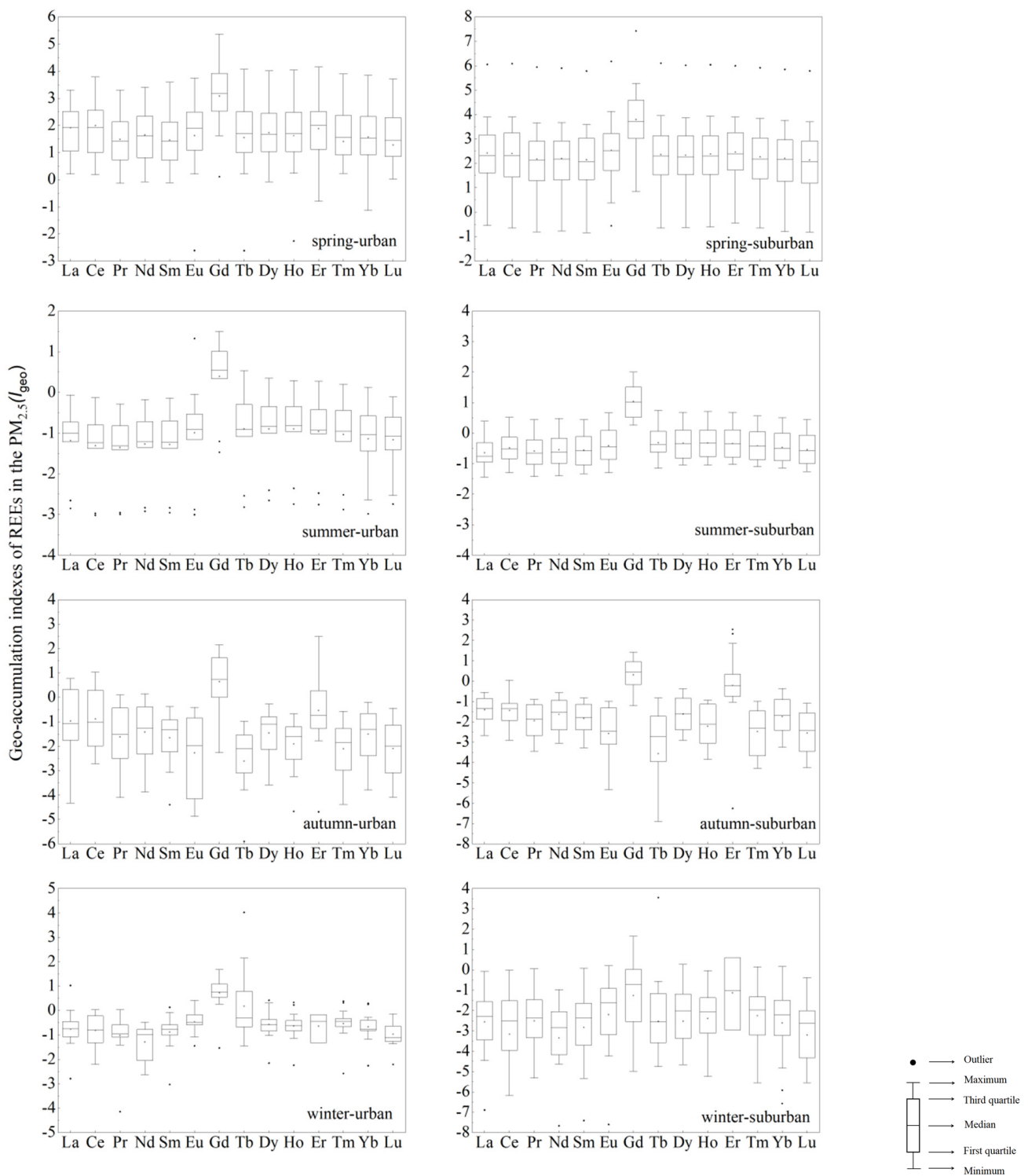


Figure 2. The I_{geo} values of REEs in $PM_{2.5}$ in Xiamen.

3.3. Distribution Patterns and Characteristic Parameters of REEs in $PM_{2.5}$

The REE distribution patterns in $PM_{2.5}$ were further used to investigate the sources of the REEs. Six Leedy chondrites [50] were used to normalize the REEs (mg/kg) in $PM_{2.5}$ samples and their potential sources in Xiamen. The enrichment of LREEs in relation to HREEs was visible in the chondrite-normalized REE patterns of all $PM_{2.5}$ samples and potential source materials (Figure 3). The distribution patterns of soil background value, coal fired dust, cement dust, waste incineration dust and road dust were similar, showing

negative Eu anomalies and a flat HREE pattern. The distribution pattern of vehicle exhaust showed positive Ce and Er anomalies and negative Eu anomalies, and the HREEs still showed a downward trend after Er. The distribution pattern of steel dust showed positive Ce and Tb anomalies, and the HREE pattern was flat as well. The firework dust showed obvious positive Eu anomalies, and firecracker dust had no obvious anomalies. In spring and summer, the REE curve of PM_{2.5} in urban and suburban areas was similar to those of the investigated potential sources, suggesting that the REEs in PM_{2.5} of urban and suburban areas mainly derive from those investigated potential sources. It was also found that PM_{2.5} samples in the autumn and winter may have been influenced by other potential non-local sources. In spring and summer, the distribution patterns of REEs in PM_{2.5} samples were similar to those of coal fired dust, background soil, cement dust and road dust. In autumn, REEs showed obviously negative Eu anomalies, and the HREE distribution showed a ‘sawtooth’ pattern, which was exactly complementary to that in Xiamen rainwater [51], this might be because typhoons were frequent in the autumn of 2018 in Xiamen and might have resulted in the soluble REEs in PM_{2.5} being washed into the biogeochemical cycle by rain [52]. In winter, the positive anomalies of Tb and the negative anomalies of Eu and Er might be influenced by vehicle exhaust and metallurgical industry in winter.

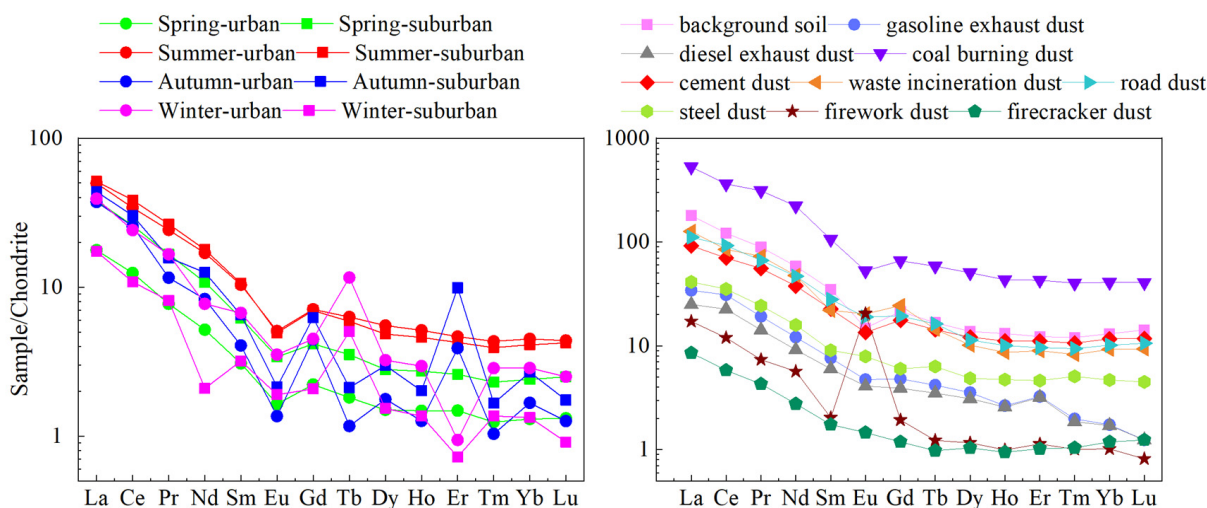


Figure 3. Chondrite-normalized REE distribution patterns in PM_{2.5} (left) and potential sources (right) in Xiamen.

The distinctive REE parameters including Ce/Ce^* , Eu/Eu^* , $\Sigma LREE/\Sigma HREE$ and $(La/Yb)_N$ were calculated to offer significant information about provenance composition (Table 2). Generally, when Ce/Ce^* (Eu/Eu^*) < 0.95, it is a negative anomaly; when Ce/Ce^* (Eu/Eu^*) > 1.05, it is a positive anomaly; and when the value ≈ 1 , there is no anomaly. $\Sigma LREE/\Sigma HREE$ and $(La/Yb)_N$ can also provide significant information about provenance composition [30]. In spring and summer, the Ce/Ce^* values showed no obvious Ce anomalies in PM_{2.5}, while Eu/Eu^* values in PM_{2.5} samples in both spring (0.65) and summer clearly demonstrated negative Eu anomalies (0.58), which was close to that of the background soil (0.54) and cement dust (0.68). In autumn, the Ce/Ce^* values showed positive anomalies, while the Eu/Eu^* values showed negative anomalies, which were similar to the case for motor vehicle exhaust dust and road dust. In winter, Ce and Eu in PM_{2.5} showed negative anomalies, which were close to those for coal burning dust and garbage incineration dust. Both $\Sigma LREE/\Sigma HREE$ and $(La/Yb)_N$ values could represent the fractionation degree between LREEs and HREEs. According to $LREE/HREE$ and $(La/Yb)_N$, the LREEs in both PM_{2.5} and potential sources were enriched in Xiamen.

Table 2. Characteristic parameters of REEs in PM_{2.5} and potential sources in Xiamen city.

		Ce/Ce* ^a	Eu/Eu* ^b	ΣLREE/ΣHREE ^c	(La/Yb) _N
PM _{2.5}	Spring	1.05	0.65	11.24	14.85
	Summer	1.01	0.58	9.80	11.81
	Autumn	1.19	0.33	10.74	19.29
	Winter	0.93	0.69	9.65	13.36
Potential sources	Background soil	0.96	0.54	11.60	13.79
	Automotive gasoline dust	1.21	0.78	11.96	19.65
	Automotive diesel dust	1.19	0.85	9.91	14.62
	Coal combustion dust	0.89	0.63	10.97	12.92
	Cement dust	0.98	0.68	7.76	7.89
	Road dust	1.07	0.82	10.14	10.95
	Waste incineration dust	0.88	0.88	9.88	13.72
	Steel dust	1.11	1.07	9.30	8.80
	Firework dust	1.06	10.33	13.98	16.98

^a Ce/Ce* = Ce_N/(La_N × Pr_N)^{0.5}. ^b Eu/Eu* = Eu_N/(Sm_N × Gd_N)^{0.5}. ^c The ratio of LREEs to HREEs.

3.4. Source Analysis of REEs by Ternary Plots

Since ternary plots could be used for the source analysis [17,53,54], the ternary La-Ce-Sm plot of PM_{2.5} and potential pollution sources in Xiamen is shown in Figure 4. Concentrations of La, Ce and Sm were adjusted to place crustal abundances of these elements in the center of the triangle. The points of the PM_{2.5} and potential source samples were all distributed near the soil background value except for firework dust, which was slightly offset to the upper right of the plot. It is noteworthy that, the distribution of PM_{2.5} was relatively concentrated in spring and summer, while it was relatively scattered in autumn and winter, indicating that the sources of PM_{2.5} samples in autumn and winter were more complex, which was consistent with the results for the distribution patterns of REEs. Additionally, the scatters of PM_{2.5} samples in the four seasons partially superposed those of the investigated potential sources samples but were not a close match, manifesting that the REEs in PM_{2.5} were influenced by other sources besides the investigated potential sources.

3.5. Nd Isotope Tracing of Rare Earth Elements in PM_{2.5}

Since Nd isotopic composition hardly changes with geochemical processes such as weathering, transportation and deposition, Nd isotopes, usually denoted by ¹⁴³Nd/¹⁴⁴Nd, have a ‘fingerprint effect’ and can be used to trace the origin of rare earth elements [55–59]. Considering that Nd isotope composition might be affected by both natural and anthropogenic sources, the relationship between Nd isotope and the characteristic parameters of REEs (Ce/Ce* and ΣLREE/ΣHREE) were analyzed to learn more about their source. The ¹⁴³Nd/¹⁴⁴Nd versus Ce/Ce* for PM_{2.5} and potential source samples are plotted in Figure 5. PM_{2.5} samples mostly fall within the ranges of cement dust, coal dust and vehicle exhaust dust in summer. The significant contribution of vehicle exhaust emissions to REEs in PM_{2.5} was also reported in Quanzhou city, which is also located in southeast China [39]. However, in autumn and winter, the points were more dispersed. The samples shifted toward the soil parent material in autumn, and most of the samples were located near the steel dust, firework dust and garbage incineration dust in winter. However, some samples were located near garbage incineration dust and road dust, indicating that the samples were affected by complex sources.

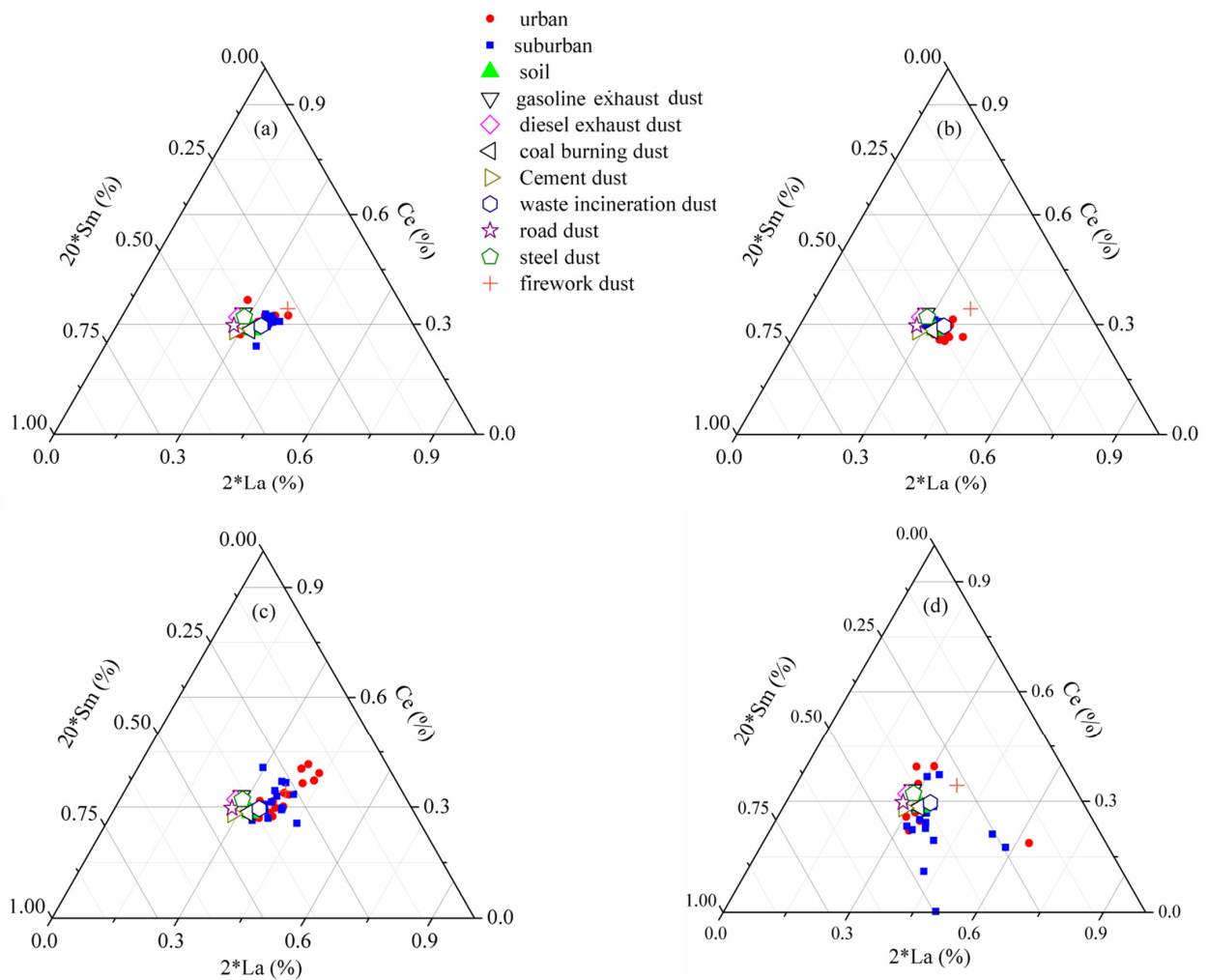


Figure 4. La-Ce-Sm ternary plots for PM_{2.5} and potential sources in Xiamen. (a–d) represent spring, summer, autumn and winter, respectively.

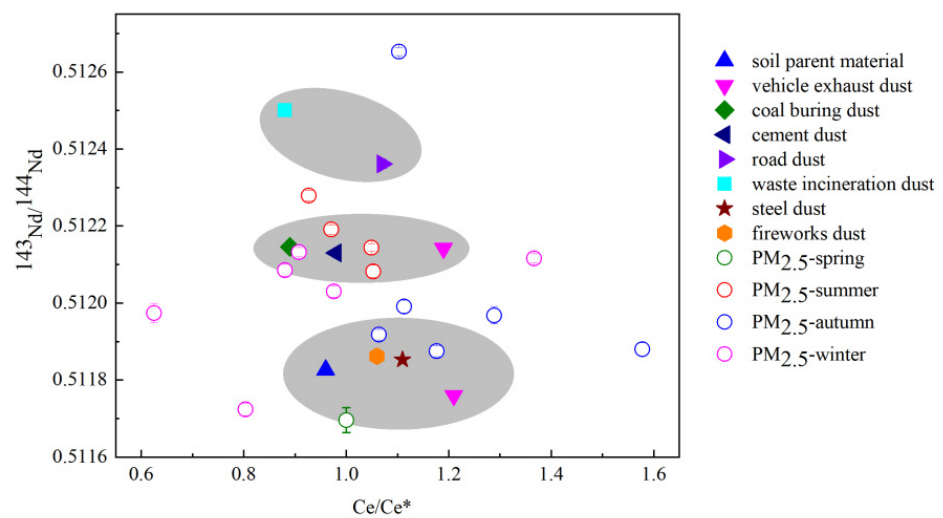


Figure 5. Relationship between Nd isotope compositions and Ce/Ce* of PM_{2.5} and potential sources in Xiamen.

4. Conclusions

The concentrations of REEs in the PM_{2.5} in Xiamen city had the order spring > autumn > winter > summer, with the LREEs ranging from 0.35 ng/m³ to 42.83 ng/m³ and the HREEs ranging from 0.03 ng/m³ to 3.56 ng/m³. In the spring and summer, the mean REE concentrations were suburban > urban, whereas in the fall and winter, they were urban > suburban. The I_{geo} values of REEs suggested possible anthropogenic effects in spring. The chondrite-normalized REE distribution patterns of the PM_{2.5} samples showed negative Eu anomalies. In the La-Ce-Sm ternary plots, the distribution of PM_{2.5} points was relatively concentrated in spring and summer, which was near the potential sources represented by soil background values, while the distribution of PM_{2.5} points was relatively scattered in autumn and winter, which shows that it was influenced by more complex factors. Furthermore, according to the ¹⁴³Nd/¹⁴⁴Nd versus Ce/Ce* plot, REEs in PM_{2.5} of Xiamen city in four seasons were affected by a variety of potential sources; vehicle exhaust emissions, coal burning dust and cement dust have a greater impact on REEs in PM_{2.5}, and the REEs sources in autumn and winter were further confirmed to be more complex than in spring and summer.

Author Contributions: Conceptualization, Y.L. and S.W.; methodology, Y.L. and Y.Y.; investigation, Y.L. and S.W.; resources, J.Y.; writing—original draft preparation, Y.L.; writing—review and editing, Y.Y., R.Y. and G.H.; supervision, Y.Y., J.Y., R.Y. and G.H.; project administration, Y.Y. and R.Y.; funding acquisition, Y.Y., R.Y. and G.H. All authors have read and agreed to the published version of the manuscript.

Funding: This research was supported by the National Natural Science Foundation of China (21477042, 21377042, 42177103), and the project was supported by the Fund of Key Laboratory of Global Change and Marine Atmospheric Chemistry, MNR, (GCMAC2006).

Institutional Review Board Statement: Not applicable.

Informed Consent Statement: Not applicable.

Data Availability Statement: The datasets generated and/or analyzed during the current study are available from the corresponding author upon reasonable request.

Conflicts of Interest: The authors declare no conflict of interest.

References

1. Huang, R.J.; Zhang, Y.; Bozzetti, C.; Ho, K.F.; Cao, J.J.; Han, Y.; Daellenbach, K.R.; Slowik, J.G.; Platt, S.M.; Canonaco, F.; et al. High secondary aerosol contribution to particulate pollution during haze events in China. *Nature* **2014**, *514*, 218–222. [[CrossRef](#)] [[PubMed](#)]
2. Sulong, N.A.; Latif, M.T.; Khan, M.F.; Amil, N.; Ashfold, M.J.; Wahab, M.I.A.; Chan, K.M.; Sahani, M. Source apportionment and health risk assessment among specific age groups during haze and non-haze episodes in Kuala Lumpur, Malaysia. *Sci. Total Environ.* **2017**, *601*, 556–570. [[CrossRef](#)] [[PubMed](#)]
3. Wei, W.; Li, Y.; Wang, Y.; Cheng, S.; Wang, L. Characteristics of VOCs during haze and non-haze days in Beijing, China: Concentration, chemical degradation and regional transport impact. *Atmos. Environ.* **2018**, *194*, 134–145. [[CrossRef](#)]
4. Dong, Z.; Su, F.; Zhang, Z.; Wang, S. Observation of chemical components of PM_{2.5} and secondary inorganic aerosol formation during haze and sandy haze days in Zhengzhou, China. *J. Environ. Sci.* **2020**, *88*, 316–325. [[CrossRef](#)] [[PubMed](#)]
5. Zeng, W.; Liu, T.; Du, Q.; Li, J.; Xiao, J.; Guo, L.; Li, X.; Xu, Y.; Xu, X.; Wan, D.; et al. The interplay of haze characteristics on mortality in the Pearl River Delta of China. *Environ. Res.* **2020**, *184*, 109279. [[CrossRef](#)]
6. Yang, S.Y.; Yu, X.Y.; Zhao, X.Y.; Li, Y.Y.; Shun, H.P.; Tian, Z.J.; Li, Y.; Wu, S.; Wang, Z.H. Characteristics of Key Size Spectrum of PM_{2.5} Affecting Winter Haze Pollution in Taiyuan. *Environ. Sci.* **2018**, *39*, 2512–2520.
7. Nakhlé, M.M.; Farah, W.; Ziade, N.; Abboud, M.; Salameh, D.; Annesi-Maesano, I. Short-term relationships between emergency hospital admissions for respiratory and cardiovascular diseases and fine particulate air pollution in Beirut, Lebanon. *Environ. Monit. Assess.* **2015**, *187*, 196. [[CrossRef](#)] [[PubMed](#)]
8. Chow, W.S.; Huang, X.H.H.; Leung, K.F.; Huang, L.; Wu, X.; Yu, J.Z. Molecular and elemental marker-based source apportionment of fine particulate matter at six sites in Hong Kong, China. *Sci. Total Environ.* **2022**, *813*, 152652. [[CrossRef](#)] [[PubMed](#)]
9. Oh, H.R.; Ho, C.H.; Kim, J.; Chen, D.; Lee, S.; Choi, Y.S.; Chang, L.S.; Song, C.K. Long-range transport of air pollutants originating in China: A possible major cause of multi-day high-PM₁₀ episodes during cold season in Seoul, Korea. *Atmos. Environ.* **2015**, *109*, 23–30. [[CrossRef](#)]

10. Wang, L.; Liu, Z.; Sun, Y.; Ji, D.; Wang, Y. Long-range transport and regional sources of PM_{2.5} in Beijing based on long-term observations from 2005 to 2010. *Atmos. Res.* **2015**, *157*, 37–48. [[CrossRef](#)]
11. Zhang, R.; Jing, J.; Tao, J.; Hsu, S.-C.; Wang, G.; Cao, J.; Lee, C.S.L.; Zhu, L.; Chen, Z.; Zhao, Y. Chemical characterization and source apportionment of PM_{2.5} in Beijing: Seasonal perspective. *Atmos. Chem. Phys.* **2013**, *13*, 7053–7074. [[CrossRef](#)]
12. Liu, B.; Wu, J.; Zhang, J.; Wang, L.; Yang, J.; Liang, D.; Dai, Q.; Bi, X.; Feng, Y.; Zhang, Y. Characterization and source apportionment of PM_{2.5} based on error estimation from EPA PMF 5.0 model at a medium city in China. *Environ. Pollut.* **2017**, *222*, 10–22. [[CrossRef](#)] [[PubMed](#)]
13. Akinlua, A.; Olise, F.S.; Akomolafe, A.O.; McCrindle, R.I. Rare earth element geochemistry of petroleum source rocks from northwestern Niger Delta. *Mar. Pet. Geol.* **2016**, *77*, 409–417. [[CrossRef](#)]
14. Atibu, E.K.; Devarajan, N.; Laffite, A.; Giuliani, G.; Salumu, J.A.; Muteb, R.C.; Mulaji, C.K.; Otamonga, J.P.; Elongo, V.; Mpiana, P.T.; et al. Assessment of trace metal and rare earth elements contamination in rivers around abandoned and active mine areas. The case of Lubumbashi River and Tshamilemba Canal, Katanga, Democratic Republic of the Congo. *Geochemistry* **2016**, *76*, 353–362. [[CrossRef](#)]
15. Zhu, B.; Ge, L.; Yang, T.; Jiang, S.; Lv, X. Stable isotopes and rare earth element compositions of ancient cold seep carbonates from Enza River, northern Apennines (Italy): Implications for fluids sources and carbonate chimney growth. *Mar. Pet. Geol.* **2019**, *109*, 434–448. [[CrossRef](#)]
16. Censi, P.; Tamburo, E.; Speziale, S.; Zuddas, P.; Randazzo, L.; Punturo, R.; Cuttitta, A.; Aricò, P. Yttrium and lanthanides in human lung fluids, probing the exposure to atmospheric fallout. *J. Hazard. Mater.* **2011**, *186*, 1103–1110. [[CrossRef](#)]
17. Zhang, H.; Feng, J.; Zhu, W.; Liu, C.; Xu, S.; Shao, P.; Wu, D.; Yang, W.; Gu, J. Chronic toxicity of rare-earth elements on human beings. *Biol. Trace Elem. Res.* **2000**, *73*, 1–17. [[CrossRef](#)]
18. Zhu, W.; Xu, S.; Shao, P.; Zhang, H.; Wu, D.; Yang, W.; Feng, J.; Feng, L. Investigation on liver function among population in high background of rare earth area in South China. *Biol. Trace Elem. Res.* **2005**, *104*, 1–7. [[CrossRef](#)]
19. McDonald, J.W.; Ghio, A.J.; Sheehan, C.E.; Bernhardt, P.F.; Roggli, V.L. Rare earth (cerium oxide) pneumoconiosis: Analytical scanning electron microscopy and literature review. *Mod. Pathol. Off. J. U. S. Can. Acad. Pathol. Inc.* **1995**, *8*, 859–865.
20. Gwenzi, W.; Mangori, L.; Danha, C.; Chaukura, N.; Dunjana, N.; Sanganyado, E. Sources, behaviour, and environmental and human health risks of high-technology rare earth elements as emerging contaminants. *Sci. Total Environ.* **2018**, *636*, 299–313. [[CrossRef](#)]
21. Wang, L.; Han, X.; Ding, S.; Liang, T.; Zhang, Y.; Xiao, J.; Dong, L.; Zhang, H. Combining multiple methods for provenance discrimination based on rare earth element geochemistry in lake sediment. *Sci. Total Environ.* **2019**, *672*, 264–274. [[CrossRef](#)] [[PubMed](#)]
22. Grousset, F.E.; Biscaye, P.E. Tracing dust sources and transport patterns using Sr, Nd and Pb isotopes. *Chem. Geol.* **2005**, *222*, 149–167. [[CrossRef](#)]
23. Grobéty, B.; Gieré, R.; Dietze, V.; Stille, P. Airborne particles in the urban environment. *Elements* **2010**, *6*, 229–234. [[CrossRef](#)]
24. Xiao, B.; Chen, H.; Hollings, P.; Han, J.; Wang, Y.; Yang, J.; Cai, K. Magmatic evolution of the Tuwu-Yandong porphyry Cu belt, NW China: Constraints from geochronology, geochemistry and Sr–Nd–Hf isotopes. *Gondwana Res.* **2017**, *43*, 74–91. [[CrossRef](#)]
25. Nakano, T.; Nishikawa, M.; Mori, I.; Shin, K.; Hosono, T.; Yokoo, Y. Source and evolution of the “perfect Asian dust storm” in early April 2001: Implications of the Sr–Nd isotope ratios. *Atmos. Environ.* **2005**, *39*, 5568–5575. [[CrossRef](#)]
26. Moragues-Quiroga, C.; Juilleret, J.; Gourdol, L.; Pelt, E.; Perrone, T.; Aubert, A.; Morvan, G.; Chabaux, F.; Legout, A.; Stille, P.; et al. Genesis and evolution of regoliths: Evidence from trace and major elements and Sr–Nd–Pb–U isotopes. *Catena* **2017**, *149*, 185–198. [[CrossRef](#)]
27. Chu, Z.Y.; Wang, M.J.; Li, C.F.; Yang, Y.H.; Xu, J.J.; Wang, W.; Guo, J.H. Separation of Nd from geological samples by a single TODGA resin column for high precision Nd isotope analysis as NdO⁺ by TIMS. *J. Anal. At. Spectrom.* **2019**, *34*, 2053–2060. [[CrossRef](#)]
28. Lee, M.K.; Lee, Y.I.; Yi, H.I. Provenances of atmospheric dust over Korea from Sr–Nd isotopes and rare earth elements in early 2006. *Atmos. Environ.* **2010**, *44*, 2401–2414. [[CrossRef](#)]
29. Yan, Y.; Yu, R.L.; Hu, G.R.; Wang, S.S.; Huang, H.B.; Cui, J.Y.; Yan, Y. Characteristics and provenances of rare earth elements in the atmospheric particles of a coastal city with large-scale optoelectronic industries. *Atmos. Environ.* **2019**, *214*, 116836. [[CrossRef](#)]
30. Yan, Y.; Zheng, Q.; Yu, R.L.; Hu, G.R.; Huang, H.B.; Lin, C.Q.; Cui, J.Y.; Yan, Y. Characteristics and provenance implications of rare earth elements and Sr–Nd isotopes in PM_{2.5} aerosols and PM_{2.5} fugitive dusts from an inland city of southeastern China. *Atmos. Environ.* **2020**, *220*, 117069. [[CrossRef](#)]
31. Pang, X.; Li, D.; Peng, A. Application of rare-earth elements in the agriculture of China and its environmental behavior in soil. *Environ. Sci. Pollut. Res.* **2002**, *9*, 143–148. [[CrossRef](#)] [[PubMed](#)]
32. Liang, T.; Li, K.; Wang, L. State of rare earth elements in different environmental components in mining areas of China. *Environ. Monit. Assess.* **2014**, *186*, 1499–1513. [[CrossRef](#)] [[PubMed](#)]
33. Dushyantha, N.; Batapola, N.; Ilankoon, I.; Rohitha, S.; Premasiri, R.; Abeysinghe, B.; Ratnayake, N.; Dissanayake, K. The story of rare earth elements (REEs): Occurrences, global distribution, genesis, geology, mineralogy and global production. *Ore Geol. Rev.* **2020**, *122*, 103521. [[CrossRef](#)]
34. Migaszewski, Z.M.; Gatuszka, A. The characteristics, occurrence, and geochemical behavior of rare earth elements in the environment: A review. *Crit. Rev. Environ. Sci. Technol.* **2015**, *45*, 429–471. [[CrossRef](#)]

35. Lin, J.; Kang, J.; Khanna, N.; Shi, L.; Zhao, X.; Liao, J. Scenario analysis of urban GHG peak and mitigation co-benefits: A case study of Xiamen City, China. *J. Clean. Prod.* **2018**, *171*, 972–983. [[CrossRef](#)]
36. Li, X.; Gao, L.; Dai, L.; Zhang, G.; Zhuang, X.; Wang, W.; Zhao, Q. Understanding the relationship among urbanisation, climate change and human health: A case study in Xiamen. *Int. J. Sustain. Dev. World Ecol.* **2010**, *17*, 304–310. [[CrossRef](#)]
37. Wang, S.; Hao, J. Air quality management in China: Issues, challenges, and options. *J. Environ. Sci.* **2012**, *24*, 2–13. [[CrossRef](#)]
38. Li, T.-C.; Chen, W.-H.; Yuan, C.-S.; Wu, S.-P.; Wang, X.-H. Physicochemical characteristics and source apportionment of atmospheric aerosol particles in Kinmen-Xiamen Airshed. *Aerosol Air Qual. Res.* **2013**, *13*, 308–323. [[CrossRef](#)]
39. Chen, J.; Qiu, S.; Shang, J.; Wilfrid, O.M.; Liu, X.; Tian, H.; Boman, J. Impact of relative humidity and water soluble constituents of PM_{2.5} on visibility impairment in Beijing, China. *Aerosol Air Qual. Res.* **2014**, *14*, 260–268. [[CrossRef](#)]
40. Deng, J.; Zhang, Y.; Hong, Y.; Xu, L.; Chen, Y.; Du, W.; Chen, J. Optical properties of PM_{2.5} and the impacts of chemical compositions in the coastal city Xiamen in China. *Sci. Total Environ.* **2016**, *557*, 665–675. [[CrossRef](#)]
41. Chang, W.; Zhan, J. The association of weather patterns with haze episodes: Recognition by PM_{2.5} oriented circulation classification applied in Xiamen, Southeastern China. *Atmos. Res.* **2017**, *197*, 425–436. [[CrossRef](#)]
42. Ma, Y.; Wang, Z.; Tan, Y.; Xu, S.; Kong, S.; Wu, G.; Wu, X.; Li, H. Comparison of inorganic chemical compositions of atmospheric TSP, PM₁₀ and PM_{2.5} in northern and southern Chinese coastal cities. *J. Environ. Sci.* **2017**, *55*, 339–353. [[CrossRef](#)] [[PubMed](#)]
43. Zhang, N.; Cao, J.; Li, L.; Ho, S.S.H.; Wang, Q.; Zhu, C.; Wang, L. Characteristics and source identification of polycyclic aromatic hydrocarbons and n-alkanes in PM_{2.5} in Xiamen. *Aerosol Air Qual. Res.* **2018**, *18*, 1673–1683. [[CrossRef](#)]
44. Wang, S.; Yan, Y.; Yu, R.; Shen, H.; Hu, G.; Wang, S. Influence of pollution reduction interventions on atmospheric PM_{2.5}: A case study from the 2017 Xiamen. *Atmos. Pollut. Res.* **2021**, *12*, 101137. [[CrossRef](#)]
45. Wang, S.; Hu, G.; Yu, R.; Shen, H.; Yan, Y. Bioaccessibility and source-specific health risk of heavy metals in PM_{2.5} in a coastal city in China. *Environ. Adv.* **2021**, *4*, 100047. [[CrossRef](#)]
46. Yang, Z.; Ruilian, Y.; Gongren, H.; Xiaohui, L.; Xianrong, L. Characteristics and environmental significance of rare earth elements in PM_{2.5} of Nanchang, China. *J. Rare Earths* **2017**, *35*, 98–106.
47. Gao, P.; Jian, H.; Xing, Y.; Tianxing, X.; Chen, X.; Jia, L.; Hang, J. Bioaccessibility and exposure assessment of PM_{2.5}-and PM₁₀-bound rare earth elements in Oil City, Northeast China. *J. Hazard. Mater.* **2020**, *396*, 122520. [[CrossRef](#)] [[PubMed](#)]
48. Hu, G.; Wang, S.; Yu, R.; Zhang, Z.; Wang, X. Source Apportionment of Rare Earth Elements in PM_{2.5} in a Southeast Coastal City of China. *Aerosol Air Qual. Res.* **2019**, *19*, 92–102. [[CrossRef](#)]
49. Muller, G. Die Schwermetallbelastung der sedimente des Neckars und seiner Nebenflüsse: Eine Bestandsaufnahme. *Chem. Ztg.* **1981**, *105*, 157–164.
50. Masuda, A.; Nakamura, N.; Tanaka, T. Fine structures of mutually normalized rare-earth patterns of chondrites. *Geochim. Cosmochim. Acta* **1973**, *37*, 239–248. [[CrossRef](#)]
51. Wang, S.-S.; Cheng, Y.-F.; Yan, J.-P.; Hu, G.-R. Distribution Characteristics and Sources of Metal Elements in Rainwater in Xiamen. *Huan Jing Ke Xue* **2019**, *40*, 4783–4790. [[PubMed](#)]
52. Yin, K.; Xu, S.; Zhu, X.; Huang, W.; Liu, S. Estimation of spatial extreme sea levels in Xiamen seas by the quadrature JPM-OS method. *Nat. Hazards* **2021**, *106*, 327–348. [[CrossRef](#)]
53. Li, K.; Liang, T.; Wang, L.; Tian, S. Inhalation exposure and potential health risk estimation of lanthanides elements in PM_{2.5} associated with rare earth mining areas: A case of Baotou city, northern China. *Environ. Geochem. Health.* **2018**, *40*, 2795–2805. [[CrossRef](#)]
54. Zhou, H.; Chun, X.; Lü, C.; He, J.; Du, D. Geochemical characteristics of rare earth elements in windowsill dust in Baotou, China: Influence of the smelting industry on levels and composition. *Environ. Sci. Processes Impacts* **2020**, *22*, 2398–2405. [[CrossRef](#)]
55. Liu, C.Q.; Masuda, A.; Okada, A.; Yabuki, S.; Fan, Z.L. Isotope geochemistry of Quaternary deposits from the arid lands in northern China. *Earth Planet. Sci. Lett.* **1994**, *127*, 25–38. [[CrossRef](#)]
56. Biscaye, P.E.; Grousset, F.E.; Revel, M.; Van der Gaast, S.; Zielinski, G.; Vaars, A.; Kukla, G. Asian provenance of glacial dust (stage 2) in the Greenland Ice Sheet Project 2 ice core, Summit, Greenland. *J. Geophys. Res. Oceans* **1997**, *102*, 26765–26781. [[CrossRef](#)]
57. Nakano, T.; Yokoo, Y.; Nishikawa, M.; Koyanagi, H. Regional Sr-Nd isotopic ratios of soil minerals in northern China as Asian dust fingerprints. *Atmos. Environ.* **2004**, *38*, 3061–3067. [[CrossRef](#)]
58. Chen, J.; Li, G.; Yang, J.; Rao, W.; Lu, H.; Balsam, W.; Sun, Y.; Ji, J. Nd and Sr isotopic characteristics of Chinese deserts: Implications for the provenances of Asian dust. *Geochim. Cosmochim. Acta* **2007**, *71*, 3904–3914. [[CrossRef](#)]
59. Rao, W.; Chen, J.; Yang, J.; Ji, J.; Li, G.; Tan, H. Sr-Nd isotopic characteristics of eolian deposits in the Erdos Desert and Chinese Loess Plateau: Implications for their provenances. *Geochem. J.* **2008**, *42*, 273–282. [[CrossRef](#)]